

Measurements of inclusive neutral diboson production with ATLAS

Cong GENG* on behalf of the ATLAS Collaboration

Department of Physics, University of Michigan, Ann Arbor, Michigan, USA

E-mail: cong.geng@cern.ch

We present recent measurements of ZZ and $Z\gamma$ production in proton-proton collisions at $\sqrt{s} = 13$ TeV with the ATLAS experiment at LHC. The unfolded differential cross section for $ZZ \rightarrow 4\ell$ as a function of the four-lepton invariant mass is presented and compared to state-of-the-art Standard Model calculations. We also report measurements of Z -boson production in association with a high-energy photon, using the Z -boson decay to neutrinos. The data in all these measurements can be used to search for triple- and quartic-neutral gauge boson interactions, which are forbidden at tree-level in the Standard Model. No excess in data is observed relative to the Standard Model expectation, and upper limits are set on the strength of $ZZ\gamma$ and $Z\gamma\gamma$ couplings.

*XXVII International Workshop on Deep-Inelastic Scattering and Related Subjects - DIS2019
8-12 April, 2019
Torino, Italy*

*Speaker.



1. Introduction

Diboson production is one of golden processes to probe the features of Standard Model (SM) and to help understand of the electroweak spontaneous symmetry breaking (EWSB). In the Run II program, the proton-proton (pp) collision at Large Hadron Collider (LHC) reached the center-of-mass energy 13 TeV and its instantaneous luminosity peaked at around $2 \times 10^{33} \text{ cm}^{-2} \text{ s}^{-1}$, providing a large amount of data to deeply study the diboson process. Among all the diboson productions, ZZ and $Z\gamma$ have clean signatures in the detector with leptonic decay final states, which enables us to disentangle the physics information based on a higher signal-to-background ratio. The report presents the recent measurements of inclusive four-lepton and $Z\gamma$ production with the data set collected at ATLAS [1] in 2015 and 2016 corresponding to an integrated luminosity of 36.1 fb^{-1} .

2. Measurement of unfolded four-lepton invariant mass spectrum at 13 TeV

In pp collisions four-lepton production is expected to receive contributions from several SM physics processes. Largest in magnitude is the quark-induced t -channel process $q\bar{q} \rightarrow 4\ell$. Gluon-induced $gg \rightarrow 4\ell$ production also occurs, via an intermediate quark loop.

The measurement of the four-lepton invariant mass ($m_{4\ell}$) spectrum is performed with selected events in the signal region containing two same-flavor opposite-sign lepton (electron or muon) pairs [2]. The electrons or muons originating from leptonic decays of the τ -lepton are not considered to be part of the signal, and their contribution to the observation at detector level is subtracted. The measurement is carried out in a fiducial phase space based on the kinematic acceptance of the detector to ensure a high selection efficiency. The fiducial phase space and all observables are defined using stable final-state particles to minimize model dependence.

The observed distributions are corrected for detector effects by an unfolding procedure. The resulting measured differential cross-section as a function of $m_{4\ell}$ is shown in Figure 1a, and compared with particle-level predictions.

Signal strength for gluon-induced 4ℓ production

The differential $m_{4\ell}$ distribution is used for this interpretation, as NLO QCD precision is available for the gluon-induced 4ℓ production in the description of this variable. The contribution from $qq \rightarrow 4\ell$ production is set to the theoretical prediction and allowed to vary within the associated theoretical uncertainties. A signal strength $\mu_{gg} = 1.3 \pm 0.5$ is measured with an expected value of 1.0 ± 0.4 . In addition, a signal strength $\mu_{gg}^{\text{LO}} = \sigma_{gg \rightarrow 4\ell}^{\text{measured}} / \sigma_{gg \rightarrow 4\ell}^{\text{SM,LO QCD}}$, is extracted relative to an uncorrected leading-order precision MCFM prediction of $gg \rightarrow 4\ell$ as $\mu_{gg}^{\text{LO}} = 2.7 \pm 0.9$, with an expected value of 2.2 ± 0.9 . This value can be compared with a previous ATLAS measurement of $\mu_{gg}^{\text{LO}} = 2.4 \pm 1.4$ performed at $\sqrt{s} = 8 \text{ TeV}$. In both cases, the uncertainty is dominated by data statistics. The largest systematic uncertainty contribution is the QCD scale choice in the $qq \rightarrow 4\ell$ prediction, and is small compared to the statistical uncertainty.

Extraction of the $Z \rightarrow 4\ell$ branching fraction

The branching fraction of $Z \rightarrow 4\ell$ is extracted using the lowest $m_{4\ell}$ bin (75–100 GeV) in the unfolded $m_{4\ell}$ distribution shown in Figure 1a. The measurement is performed in an extended phase

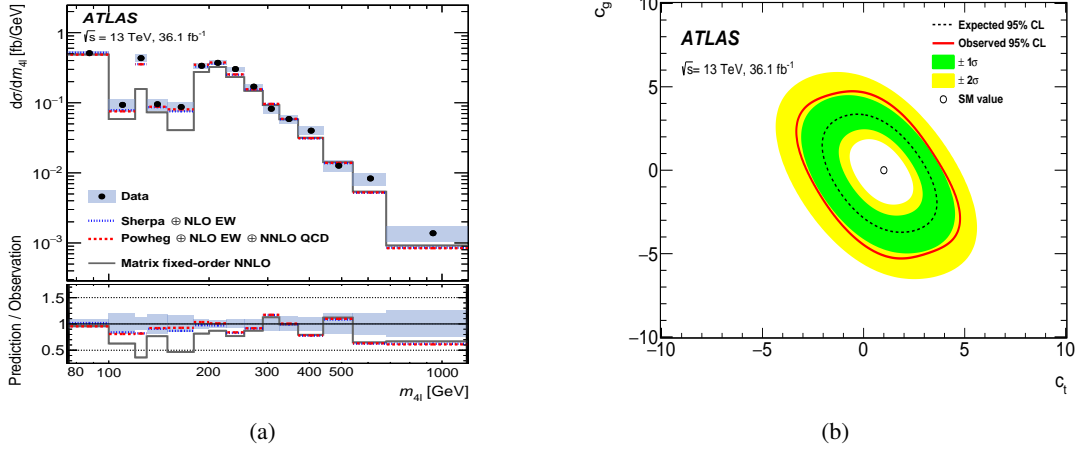


Figure 1: (a) is the measured differential cross-section (black dots) compared with particle-level SM predictions (colored lines) for the $m_{4\ell}$ distribution. Two SM predictions with different event generator samples for $qq \rightarrow 4\ell$ are shown with different line colors and styles. (b) is observed (solid) and expected (dashed) exclusion limits at 95% CL in the c_g versus c_t plane for modified $t\bar{t}H$ and ggH couplings. The uncertainties in the expected limit corresponding to one and two standard deviations are displayed as green and yellow bands respectively. The hollow circle denotes the tree-level SM values of the parameters: $c_g = 0$ and $c_t = 1$ [2].

space defined by values of the invariant mass of the four-lepton system $m_{4\ell}$ and the lowest dilepton invariant mass in the event, $m_{\ell\ell}$, satisfying $80 < m_{4\ell} < 100$ GeV and $m_{\ell\ell} > 4$ GeV. The branching fraction is then calculated as:

$$\mathcal{B}_{Z \rightarrow 4\ell} = \frac{N_{\text{fid}} \times (1 - f_{\text{non-res}})}{\sigma_Z \times A_{\text{fid}} \times \mathcal{L}},$$

where N_{fid} is the number of unfolded events in this bin, A_{fid} is the fiducial acceptance, σ_Z is the total cross-section for single Z production, \mathcal{L} is the integrated luminosity, and $f_{\text{non-res}}$ is the fraction of non-resonant events in the extended phase space, calculated using POWHEG-BOX. The acceptance (including the non-resonant contribution) is calculated using MC simulation as $A_{\text{fid}} = (4.75 \pm 0.02)\%$ and the fraction of non-resonant events as $f_{\text{non-res}} = (4.8 \pm 0.5)\%$.

This result is compared with previous dedicated measurements by the ATLAS [3] and CMS [4] collaborations in Table 1. The largest contributing systematic uncertainties in this mass region come from lepton identification and reconstruction efficiencies. The difference in systematic uncertainties compared to Ref. [3] is due to the assumptions of non-correlation between uncertainties in the two contributing measurements discussed above. The larger statistical uncertainty compared to Ref. [4] arises from an acceptance which has not been fully optimized for this interpretation.

Constraint on modified Higgs boson couplings

The detector-corrected four-lepton mass distribution is used to constrain possible BSM modifications of the couplings of the Higgs boson to top quarks (c_t) and gluons (c_g , zero in the SM) [5]. On-shell rates for Higgs production via gluon-gluon fusion are only sensitive to $|c_t + c_g|^2$, but

Table 1: Comparison of measurements for the $Z \rightarrow 4\ell$ branching fraction in the phase-space region $80 \text{ GeV} < m_{4\ell} < 100 \text{ GeV}$, $m_{\ell\ell} > 4 \text{ GeV}$.

Measurement	$\mathcal{B}_{Z \rightarrow 4\ell} / 10^{-6}$
ATLAS, $\sqrt{s} = 7 \text{ TeV}$ and 8 TeV [3]	$4.31 \pm 0.34(\text{stat}) \pm 0.17(\text{syst})$
CMS, $\sqrt{s} = 13 \text{ TeV}$ [4]	$4.83^{+0.23}_{-0.22}(\text{stat})^{+0.32}_{-0.29}(\text{syst}) \pm 0.08(\text{theo}) \pm 0.12(\text{lumi})$
ATLAS, $\sqrt{s} = 13 \text{ TeV}$	$4.70 \pm 0.32(\text{stat}) \pm 0.21(\text{syst}) \pm 0.14(\text{lumi})$

measurements at higher mass ($> 180 \text{ GeV}$) can be used to probe these parameters independently, as the partonic centre-of-mass energy of the process becomes larger than the top-quark mass. This provides an interesting test of the off-shell behavior beyond dedicated measurements based on the rare $t\bar{t}H$ production mode. Again, the yield from $q\bar{q} \rightarrow 4\ell$ is set to the Standard Model prediction and allowed to float within the associated theoretical uncertainties, while the yield from $g\bar{g} \rightarrow 4\ell$ is parameterized as a function of c_t and c_g using the procedure described in Ref. [5]. The observed and expected 95% CL exclusion contours obtained using the CL_s method are shown in Figure 1b.

Exclusion limits were also explored for a model of anomalous triple gauge couplings considered in a dedicated search region of the ATLAS on-shell $ZZ \rightarrow 4\ell$ measurement [6]. Here, it was found that the present detector-corrected analysis is far less sensitive. This is a general feature of cross-section measurement reinterpretations in terms of models with effects that appear in the very poorly populated tails of distributions: the statistical requirements of unfolding mean that bins will need to be wide in these regions, and therefore sensitivity will be decreased.

3. Measurement of $Z\gamma$ production with $Z \rightarrow \nu\nu$ at 13 TeV

The measurement of $Z\gamma$ production is performed with the Z boson decaying into neutrinos [7]. The measurements are made both with no restriction on the system recoiling against the $Z\gamma$ pair and by requiring that no jets with $|\eta| < 4.5$ and $p_T > 50 \text{ GeV}$ are present in addition to the $Z\gamma$ pair. The $\nu\bar{\nu}\gamma$ final state in the SM can be produced by a Z boson decaying into neutrinos in association with photon emission from initial-state quarks or from quark/gluon fragmentation. The neutral triple gauge-boson couplings are forbidden at tree level in the SM but can arise in theories that extend the SM.

The measured cross sections for $Z(\nu\bar{\nu})\gamma$ production in the extended fiducial region are $83.7^{+3.6}_{-3.5}$ (stat.) $^{+6.9}_{-6.2}$ (syst.) $^{+1.7}_{-2.0}$ (lumi.) in the inclusive $N_{\text{jets}} \geq 0$ and $52.4^{+2.4}_{-2.3}$ (stat.) $^{+4.0}_{-3.6}$ (syst.) $^{+1.2}_{-1.1}$ (lumi.) in the exclusive $N_{\text{jets}} = 0$ extended fiducial regions. The measured cross sections agree with the SM expectations from MCFM generator, $78.1 \pm 0.2(\text{stat.}) \pm 4.7(\text{syst.})$ for the inclusive $N_{\text{jets}} \geq 0$ and $55.9 \pm 0.1(\text{stat.}) \pm 3.9(\text{syst.})$ for the exclusive $N_{\text{jets}} = 0$, respectively, within one standard deviation. Compared with the $Z\gamma$ measurements at $\sqrt{s} = 8 \text{ TeV}$, the systematic uncertainty is significantly reduced. This improvement is due primarily to the reduction of systematic uncertainty allowed by the data-driven estimate of the γ +jets and $W\gamma$ backgrounds. The differential cross sections as a function of E_T^γ are shown in Figure 2 for both the inclusive and exclusive measurements.

The yields of $Z\gamma$ events with high E_T^γ from the exclusive (zero-jet) selection are used to set limits on parameters $h_{3,4}^V$, which parameterize the anomalous triple gauge-boson coupling contributions to $Z\gamma$ production within the framework of the effective vertex function approach. The

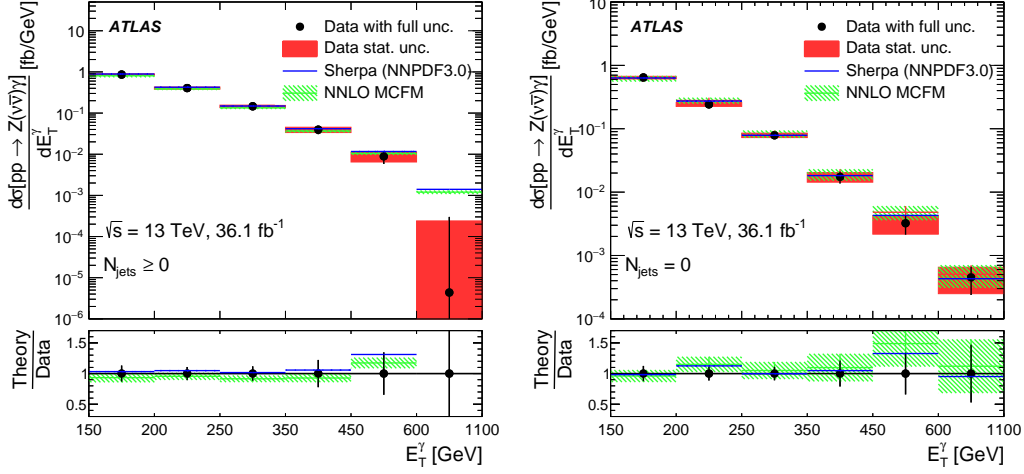


Figure 2: The measured (points with error bars) and predicted differential cross sections as a function of E_T^γ for the $pp \rightarrow Z(\nu\bar{\nu})\gamma$ process in the inclusive $N_{\text{jets}} \geq 0$ (left) and exclusive $N_{\text{jets}} = 0$ (right) extended fiducial regions. The error bars on the data points show the sum in quadrature of the statistical and systematic uncertainties. The MCFM NNLO predictions are shown with shaded bands that indicate the theoretical uncertainties. For the SHERPA predictions, systematic uncertainties are not considered, and the statistical uncertainties arising from the size of the MC samples are too small to be visible [7].

	Limit 95% CL			Limit 95% CL	
	Measured [10^{-4}]	Expected [10^{-4}]		Measured [TeV^{-4}]	Expected [TeV^{-4}]
h_3^γ	(-3.7, 3.7)	(-4.2, 4.3)	$C_{\tilde{B}W}/\Lambda^4$	(-1.1, 1.1)	(-1.3, 1.3)
h_3^Z	(-3.2, 3.3)	(-3.8, 3.8)	C_{BW}/Λ^4	(-0.65, 0.64)	(-0.74, 0.74)
h_4^γ	(-4.4, 4.3)	(-5.1, 5.0)	C_{WW}/Λ^4	(-2.3, 2.3)	(-2.7, 2.7)
h_4^Z	(-4.5, 4.4)	(-5.3, 5.1)	C_{BB}/Λ^4	(-0.24, 0.24)	(-0.28, 0.27)

Table 2: Observed and expected one-dimensional 95% CL limits on (left-hand side table) h_3^γ , h_3^Z , h_4^γ and h_4^Z , (right-hand side table) $C_{\tilde{B}W}/\Lambda^4$, C_{BW}/Λ^4 , C_{WW}/Λ^4 and C_{BB}/Λ^4 EFT parameters. For each row, all parameters other than the one under study are set to 0.

exclusive selection is used because it significantly reduces the SM contribution at high E_T^γ and therefore optimizes the sensitivity to anomalous couplings. The contribution from aTGCs increases with the E_T of the photon, and the measurement of $Z\gamma$ production is found to have the highest sensitivity to aTGCs by restricting the search to the portion of the extended fiducial region with E_T^γ greater than 600 GeV.

No evidence of anomalous couplings is observed. The allowed 95% CL ranges for the anomalous couplings are shown in the left-hand side of Table 2 for $ZZ\gamma$ (h_3^Z and h_4^Z) and the $Z\gamma\gamma$ (h_3^γ and h_4^γ) vertices. Limits on anomalous couplings imposed by this analysis are 3–7 times more stringent than those from prior studies [8].

Allowed ranges are also determined for parameters of the effective field theory (EFT), which includes four dimension-8 operators describing aTGC interactions of neutral gauge bosons. The coefficients of these operators are denoted $C_{\tilde{B}W}/\Lambda^4$, C_{BW}/Λ^4 , C_{WW}/Λ^4 and C_{BB}/Λ^4 , as described in Ref. [10]. The parameter Λ has the dimension of mass and is associated with the energy scale of the new physics described by the EFT. The 95% CL limits on these EFT parameters displayed in the right-hand side of Table 2 are derived from the limits of left-hand side of Table 2 making use of a linear transformation relating the EFT and vertex function aTGC parameters, obtained from Ref. [10].

4. Summary

The report presents the recent measurements of inclusive four-lepton invariant mass and $Z\gamma$ production with the data set collected at ATLAS in the Run II of LHC in 2015 and 2016 corresponding to an integrated luminosity of 36.1 fb^{-1} . In the results, we report the measurements of the integrated and differential cross sections and the comparison to state-of-the-art SM calculations, as well as the beyond SM (BSM) searches.

References

- [1] ATLAS Collaboration, *The ATLAS Experiment at the CERN Large Hadron Collider*, JINST **3** (2008) S08003
- [2] ATLAS Collaboration, *Measurement of the four-lepton invariant mass spectrum in 13 TeV proton-proton collisions with the ATLAS*, JHEP **04** (2019) 048, arXiv:1902.05892.
- [3] ATLAS Collaboration, *Measurements of Four-Lepton Production at the Z Resonance in pp Collisions at $\sqrt{s} = 7$ and 8 TeV with ATLAS*, Phys. Rev. Lett. **112** (2014) 231806, arXiv:1403.5657.
- [4] CMS Collaboration, *Measurements of the $pp \rightarrow ZZ$ production cross section and the $Z \rightarrow 4\ell$ branching fraction, and constraints on anomalous triple gauge couplings at $\sqrt{s} = 13$ TeV*, Eur. Phys. J. C **78** (2018) 165, Erratum: Eur. Phys. J. C **78** (2018) 515, arXiv:1709.08601.
- [5] Aleksandr Azatov, Christophe Grojean, Ayan Paul, Ennio Salvioni, *Taming the off-shell Higgs boson* J. Exp. Theor. Phys. **120** (2015) 354, ssn: 1090-6509, arXiv:1406.6338.
- [6] ATLAS Collaboration, *$ZZ \rightarrow \ell^+ \ell^- \ell'^+ \ell'^-$ cross-section measurements and search for anomalous triple gauge couplings in 13 TeV pp collisions with the ATLAS detector*, Phys. Rev. D **97** (2018) 032005, arXiv:1709.07703.
- [7] ATLAS Collaboration, *Measurement of the $Z\gamma \rightarrow \nu\bar{\nu}\gamma$ production cross section in pp collisions at $\sqrt{s} = 13$ TeV with the ATLAS detector and limits on anomalous triple gauge-boson couplings*, JHEP **12** (2018) 010, arXiv:1810.04995.
- [8] ATLAS Collaboration, *Measurements of $Z\gamma$ and $Z\gamma\gamma$ production in pp collisions at $\sqrt{s} = 8$ TeV with the ATLAS detector*, Phys. Rev. D **93** (2016) 112002, arXiv:1604.05232.
- [9] U. Baur and E. L. Berger, *Probing the weak-boson sector in $Z\gamma$ production at hadron colliders* Phys. Rev. D **47** (1993) 4889.
- [10] Celine Degrande, *A basis of dimension-eight operators for anomalous neutral triple gauge boson interactions*, JHEP **1402** (2014) 101, arXiv:1308.6323.